Simple model for vibration-translation exchange at high temperatures: Effects of multiquantum transitions on the relaxation of a N_2 gas flow behind a shock

A. Aliat,[1,*] P. Vedula,[1,*] and E. Josyula[2]

[1]*School of Aerospace and Mechanical Engineering, University of Oklahoma, Norman, Oklahoma 73019, USA*

[2]*US Air Force Research Laboratory, Wright-Patterson Air Force Base, Dayton, Ohio 45433, USA*

(Received 13 September 2010; revised manuscript received 3 November 2010; published 22 February 2011)

In this paper a simple model is proposed for computation of rate coefficients related to vibration-translation transitions based on the forced harmonic oscillator theory. This model, which is developed by considering a quadrature method, provides rate coefficients that are in very good agreement with those found in the literature for the high temperature regime ($\gtrsim$10 000 K). This model is implemented to study a one-dimensional nonequilibrium inviscid N_2 flow behind a plane shock by considering a state-to-state approach. While the effects of ionization and chemical reactions are neglected in our study, our results show that multiquantum transitions have a great influence on the relaxation of the macroscopic parameters of the gas flow behind the shock, especially on vibrational distributions of high levels. All vibrational states are influenced by multiquantum processes, but the effective number of transitions decreases inversely according to the vibrational quantum number. For the initial conditions considered in this study, excited electronic states are found to be weakly populated and can be neglected in modeling. Moreover, the computing time is considerably reduced with the model described in this paper compared to others found in the literature.

DOI: 10.1103/PhysRevE.83.026308 PACS number(s): 47.70.Nd, 34.50.Ez, 82.20.Rp

I. INTRODUCTION

Nonequilibrium vibrational kinetics at high temperature is a topic of interest in hypersonic aerodynamics studies [1]. One-temperature and multitemperature models that are widely used in the literature to simulate hypersonic gas flows are based on the assumption of quasistationary distributions (Boltzmann or Treanor) over vibrational energies [2–5]. These quasistationary distributions are valid if characteristic mean times related to vibration-translation (VT), vibration-vibration (VV), and chemical reactions differ by many orders of magnitude. In particular, the one-temperature models assume significantly faster vibrational energy exchanges compared to chemical reactions, while multitemperature models assume rapid VV and slow VT processes. However, more accurate rate coefficients calculated for VT, VV [6–10], and dissociation processes [10,11] show that their respective characteristic times are not very different from each other for a wide range of temperatures. Due to this observation, one-temperature and multitemperature models can be deemed to be inadequate and hence more detailed state-to-state kinetic models are needed.

The main advantage of the state-to-state kinetic approach is that the population densities of vibrational quantum states are directly predicted, without the use of assumptions of any quasistationary distributions. Recently, many studies have been carried out with the state-to-state approach such as in high temperature N_2, O_2, and CO gas flows behind shock waves [12–17], expanding flows in nozzles [18–22], and flows in boundary layers [23,24] and near blunt bodies [25–27]. Transport coefficients based on state-to-state kinetics were developed in Ref. [28] and results show a significant influence of nonequilibrium vibrational distributions on the heat transfer. Radiative processes are also taken into account in Ref. [29] and numerical applications [16,17] have shown evidence of the strong coupling between the physicochemical and radiative processes. This strong coupling leads to the conclusion that the common local thermal equilibrium (LTE) assumption often used to treat radiative mechanisms [30–32], can result in significant errors in the evaluation of the radiation and the radiative heat issued by gas flows. Also, it was shown that excited electronic states can strongly influence the evolution of the macroscopic parameters of the gas flow behind a shock [16,17].

Densities of vibrational levels are initially governed by source terms related to VV and VT collisions in master equations. However, it was shown that VV mechanisms can be neglected at high temperatures (over $\sim$10 000 K) for N_2 and CO molecules [16,33] and hence VT transitions are dominant in vibrational energy exchanges. In this study we focus on the effects of pure VT multiquantum transitions, while neglecting the effects of radiation, ionization, dissociation, recombination, and other chemical reactions which will be systematically included in future studies. Although the latter effects are important at high temperatures, the strong dependence of their rates on the nonequilibrium vibrational population levels necessitates accurate modeling of vibrational energy exchanges. For instance, dissociation of diatomic molecules, which is significant at high temperatures, proceeds preferentially from vibrational levels close to the dissociation energy, so that the vibrational nonequilibrium affects the dissociation rate. Dissociation and the vibrational relaxation are thus strongly coupled, and hence accurate modeling of diatomic gases requires a careful description of vibrational nonequilibrium to determine the degree of dissociation in the flow field.

Modeling of state-specific rate coefficients for vibrational energy exchanges is widely discussed in the literature. Although semiclassical calculations for three-dimensional collisions [6–8] and the exact quantum approach [9,10] provide good accuracy, they remain nevertheless computationally very expensive. However, the above accurate calculations are often

*Corresponding authors: azizaliat@ou.edu; pvedula@ou.edu.

used to fit the parameters in approximate approaches [34–36] which are commonly used because of their simplicity and low computing time. The rate coefficients utilized in computational fluid dynamics (CFD) codes are often dependent of the translational temperature alone. The most popular model of vibrational energy exchanges is that of Schwartz, Slawsky, and Herzfeld (SSH) [37], which is based on a semiclassical first-order perturbation theory (FOPT). This model is developed for a collinear binary collision characterized by an exponential repulsive potential interaction; its generalization for anharmonic oscillators is given in Refs. [38,39]. However, it is known that the SSH model works rather well for low quantum vibrational levels but fails at high collision velocities and high quantum numbers and cannot be applied for multiquantum jumps. To avoid these limits of application, a more rigorous theoretical approach is proposed on the basis of a nonperturbative forced harmonic oscillator (FHO) [40–42] also assuming a collinear binary collision. The FHO approach takes into account the coupling of many vibrational states during a collision, which can be valid in high temperature conditions and for multiquantum transitions. Adamovich *et al.* [43] extended the FHO model by including the anharmonicity of molecules and a steric factor to take into account the noncollinear nature of collisions. The steric factor is obtained from interpolations of experimental measurements or more accurate calculations. However, the direct use of FHO analytical expressions leads to numerical singularities and VT transition probabilities greater than unity at high vibrational quantum numbers [44,45]. Nevertheless under such conditions, the analytical expressions for the VT rate coefficients can be obtained using the model proposed by Nikitin and Osipov [46]. This asymptotic model uses properties of Bessel functions and appears to be valid for all vibrational quantum numbers and a large range of temperature [16,17,43].

However, it should be noted that VT rate coefficients are obtained by averaging transition probabilities over relative collision velocities via a distribution function. This average calculation is required for each transition and each temperature, which can lead to a great computing time to obtain rate coefficients in master equations. For this reason, the assumption of monoquantum collisions is commonly used and molecules remain in their ground electronic states to limit the number of VT transitions. An analytical model which can provide satisfactory FHO rate coefficients with a similar computing time as the SSH model could greatly facilitate and extend numerical applications of the state-to-state approach for modeling gas flows at high temperatures.

In this paper, we propose a model which approximates that of Nikitin and Osipov [46] by considering properties of Bessel functions. Then, a quadrature method is utilized to calculate FHO rate coefficients related to VT transitions with a shorter computing time. To bring out the advantages of the proposed approach, the rate coefficients of both multiquantum and monoquantum transitions calculated on the basis of the approximate model and that of Nikitin and Osipov are implemented to study a one-dimensional nonequilibrium inviscid N_2 gas flow behind a plane shock. Numerical results obtained from these two models in the context of relaxation of the gas flow macroscopic parameters are discussed. The significance of multiquantum transitions in the vibrational nonequilibrium description is evaluated and the underlying effects are compared to those obtained based on the restricted assumption of monoquantum transitions, which is widely used in the literature. Finally, computing times consumed by considering various VT models are estimated and compared.

II. FHO MODELS

A VT transition can be described by the following process:

$$A_{\alpha,i} + M \leftrightarrow A_{\alpha,i'} + M, \tag{1}$$

where the terms α and i correspond to the electronic and vibrational states of a diatomic molecule A, respectively. As the result of VT collisional interaction with its partner M (atom or molecule), the molecule A is found on a different vibrational level i' $(\neq i)$.The gap of vibrational energy $\Delta\varepsilon$ involved during this vibrational jump is shared with the translational mode of the molecule and its collisional partner, which is why the above process is called a vibration-translation transition. In this study, both monoquantum $(|i - i'| = 1)$ and multiquantum $(|i - i'| > 1)$ transitions are considered.

The FHO transition probability related to the mechanism Eq. (1) is derived by Adamovich *et al.* [43] and given by

$$P_{ii'}^{VT}(v_0) = i!i'!\varepsilon^{i+i'}\exp(-\varepsilon)\left|\sum_{r=0}^{n}\frac{(-1)^r}{r!(i-r)!(i'-r)!}\frac{1}{\varepsilon^r}\right|^2, \tag{2}$$

where $n = \min(i,i')$, and ε is the average number of quanta transmitted to the initially nonvibrating oscillator, such as

$$\varepsilon(v_0) = \frac{4\pi^3\omega}{\alpha^2\mu h}\left(\frac{\tilde{m}\gamma}{\alpha}\right)^2\sinh^{-2}\left(\frac{\pi\omega}{\alpha\bar{v}}\right). \tag{3}$$

Terms $\omega(= 2\pi\Delta\varepsilon/h)$ and h are the angular frequency and the Planck's constant, respectively. The symmetrized relative collision velocity $\bar{v}[= (v_0 + v_0')/2]$ takes into account the detailed balance and the total energy conservation during the VT interaction. The final relative collision velocity v_0' is connected to the initial velocity v_0 $(v_0' = \sqrt{v_0^2 + 2\Delta\varepsilon/\tilde{m}})$. The expression Eq. (3) is obtained on the basis of the repulsive exponential interaction potential $V(r) \sim \exp(-\alpha r)$ and its mass parameters ($\tilde{m}$, γ,and μ) are given in Ref. [43]. Moreover, the expression Eq. (3) is multiplied by a steric factor S_{VT} to take into account the noncollinear nature of collisions and is considered to be an adjustable parameter. In this study, we adopt the value of 4/9 proposed by Adamovich *et al.* [43] for N_2-N_2 collisional interactions. This value is obtained from matching the above FHO transition probabilities at relatively low velocities with more accurate probabilities of Billing and Fisher [6]. Indeed, the latter authors performed calculations for three-dimensional collisions with a more realistic intermolecular potential.

However, the transition probability Eq. (2) cannot be used for vibrational energy exchange at high vibrational levels. Indeed, factorial calculations cannot be done accurately since numerical singularities (overflows and underflows) appear for high vibrational levels and unphysical transition probabilities

are obtained [44,45]. For the high states, the following asymptotic model of Nikitin and Osipov [46] is suggested:

$$P_{ii'}^{VT}(v_0) = J_s^2(x_s), \tag{4}$$

where $x_s(v_0) = 2\sqrt{n_s \varepsilon}$ is introduced to facilitate the notation in the next section of the paper. The term J_s represents the Bessel function of the first kind at the sth order, while $s = |i - i'|$ and $n_s = [\max(i,i')!/\min(i,i')!]^{1/s}$.

The rate coefficients $k_{ii'}^{VT}$ are obtained by averaging transition probabilities $P_{ii'}^{VT}$ given by Eqs. (2) and (4) over initial relative velocities as follows:

$$k_{ii'}^{VT}(T) = Z_M^{\text{coll}}(T) \int_0^\infty f_M^{\text{dist}}(v_0,T) P_{ii'}^{VT}(v_0)\, dv_0, \tag{5}$$

where the one-dimensional Maxwellian speed distribution function and the gas-kinetic frequency are given by [47]

$$f_M^{\text{distr}}(v_0,T) = \left(\frac{\tilde{m}}{kT}\right) v_0 \exp\left(-\frac{\tilde{m} v_0^2}{2kT}\right) \tag{6}$$

and

$$Z_M^{\text{coll}}(T) = \sigma \sqrt{\frac{8\pi kT}{\tilde{m}}}, \tag{7}$$

respectively. Note that the above two expressions depend on the translational temperature T and are related to the collision partner M. The term σ is the collision diameter where chemical species are considered as hard spheres.

It is obvious that the direct calculation of the integral in Eq. (5) over initial relative collision velocities can involve significant computational costs (i.e., time) in fluid dynamics simulations. Indeed, the integral is computed at each variation of temperature for each VT transition. The number of VT transitions is proportional to the number of vibrational levels and can be very high. In the next section an approximate model is proposed to obtain via the FHO model the rate coefficients and reduce greatly the computing time. This model is based on a quadrature method and uses properties of Bessel functions.

III. APPROXIMATE FHO MODEL

The Bessel function $J_s(x_s)$ in Eq. (4) is an oscillatory function and can be evaluated by its asymptotic functions $J_{1,s}$ and $J_{2,s}$ [48]. The use of these two functions allows us to approximate arbitrarily the VT transition probability Eq. (4) of Nikitin and Osipov [46] in three ranges of application as follows:

$$P_{ii'}^{VT}(v_0) \sim \begin{cases} J_{1,s}^2(x_s) = \left[\frac{1}{s!}\left(\frac{x_s}{2}\right)^s\right]^2, & x_s \in [0, x_{1,s}], \\ J_{1,s}^2(x_{1,s}) = J_{2,s}^2(x_{2,s}), & x_s \in [x_{1,s}, x_{2,s}], \\ J_{2,s}^2(x_s) = \frac{2}{\pi x_s}\cos^2\left[x_s - (2s+1)\frac{\pi}{4}\right], & x_s \in \left[x_{2,s}, \infty\right), \end{cases} \tag{8}$$

The main advantage of the above formulation is that we can evaluate the characteristics of peaks described by the square of the Bessel's function in the Nikitin and Osipov expression Eq. (4). Indeed, by considering the kth peak, it is easy to see

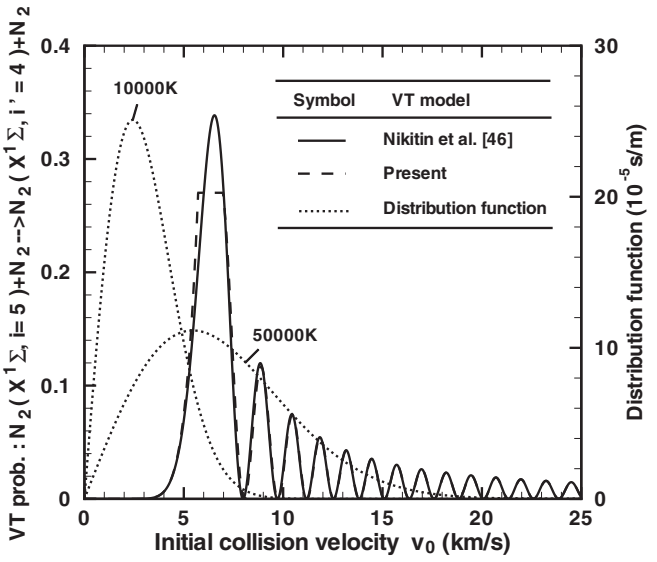

FIG. 1. Monoquantum VT transition probability related to $N_2(X\,^1\Sigma, i = 5) + N_2 \rightarrow N_2(X\,^1\Sigma, i' = 4) + N_2$ process and the collisional distribution function (for 10 000 and 50 000 K), both as functions of the initial relative velocity v_0. Various VT models are considered.

in $[x_{2,s}, \infty)$ that its central position $x_{2,s,k}$ and its height $h_{2,s,k}$ are given by

$$x_{2,s,k} = (2s+1)\pi/4 + (k-1)\pi \tag{9}$$

and

$$h_{2,s,k} = 2/(\pi x_{2,s,k}), \tag{10}$$

respectively. The component $x_{1,s}$ in Eq. (8) describes the position of $J_{1,s}$ when it reaches a magnitude equal to the height of the first peak located at its central position $x_{2,s,k=1}$, i.e., $J_{1,s}^2(x_{1,s}) = J_{2,s}^2(x_{2,s,k=1})$. Under this condition, the component $x_{1,s}$ is given by

$$x_{1,s} = 2\left(\frac{2s!}{\pi(s+1/2)^{1/2}}\right), \tag{11}$$

while asymptotic functions $J_{1,s}$ and $J_{2,s}$ are directly linked in the $[x_{1,s}, x_{2,s}]$ range.

Figure 1 shows the transition probability related to the monoquantum process $N_2(X\,^1\Sigma, i = 5) + N_2 \rightarrow N_2(X\,^1\Sigma, i' = 4) + N_2$. Note that $X\,^1\Sigma$ corresponds to the ground electronic state of N_2 molecules and monoquantum transitions involve the Bessel function at the first order ($s = 1$). In this figure, we can see that higher peaks ($k > 1$) of the Nikitin and Osipov model Eq. (4) are well described by the approximate form Eq. (8) in $[x_{2,s=1}, \infty)$. We approximate the first peak ($k = 1$) of the Nikitin and Osipov model using the asymptotic functions $J_{1,s=1}$ and $J_{2,s=1}$ (illustrated by dashed lines) on the left and right slopes (respectively) of the first peak, which are bridged using a constant (plateau) value in the central region $[x_{1,s}, x_{2,s}]$ of the peak. The constant value is chosen to correspond to the extremum of $J_{2,s=1}$ located at $x_{2,s=1}$.

The presence of the peaks allows us to split the integral in Eq. (5) and obtain the following expression:

$$k_{ii'}^{VT}(T) = Z_M^{\text{coll}}(T) \sum_k I_k \tag{12}$$

with

$$I_k = \int_{\Delta v_k} f_{AM}^{\text{distr}}(v_0,T) P_{ii'}^{VT}(v_0) dv_0, \tag{13}$$

and where the term Δv_k corresponds to the velocity range at the end points of the kth peak. Moreover, we can observe in Fig. 1 that the collisional distribution function covers more peaks ($k > 1$) at higher temperatures (as at 50 000 K). Note that since the peaks are rather sharp, we can assume that the magnitude of the distribution function varies slowly within them. So, in the first approximation we can assume that this magnitude is constant and equal to that on the central velocity $v_{2,s,k}$ within each peak k; the central velocity along the v_0 axis corresponds to the above central position $x_{2,s,k}$ along the x_s axis. The assumption of slow variation committed by the distribution function allows us to rewrite Eq. (13) as follows:

$$I_k \sim f_M^{\text{distr}}(v_{2,s,k},T) \int_{\Delta v_k} P_{ii'}^{VT}(v_0) dv_0, \tag{14}$$

where the integral bound on the Δv_k range is simply the calculation of the area related to the kth peak. The surface of this peak can be estimated by the method of "triangles" [49], i.e., by multiplying its height $h_{2,s,k}$ by its width at the half height $\Delta v'_k$. Thus, the relation Eq. (14) becomes

$$I_k \sim f_M^{\text{distr}}(v_{2,s,k},T) P_{ii'}^{VT}(v_{2,s,k}) \Delta v'_k. \tag{15}$$

Finally, introducing the above relation in Eq. (12), we can estimate the general VT rate coefficients Eq. (5) by a quadrature method as follows:

$$k_{ii'}^{VT}(T) \sim Z_M^{\text{coll}}(T) \left[I_{k=1} + \sum_{k>1} f_M^{\text{distr}}(v_{2,s,k},T) \times P_{i,f}^{VT}(v_{2,s,k}) \Delta v'_k \right]. \tag{16}$$

However, Fig. 1 shows that the first peak ($k = 1$) is larger than the others and that the assumption of slow variation of the collisional distribution function within this peak is not justified, especially at lower temperatures (as at 10 000 K). To maintain the goal of reducing computing time without loss of accuracy in calculations at high temperatures, in the first approximation we split the integral $I_{k=1}$ Eq. (13) over the three ranges of application of the approximate transition probability Eq. (8) as follows:

$$I_{k=1} = \int_{x_{0,1}}^{x_{1,s}} + \int_{x_{1,s}}^{x_{2,s}} \int_{x_{2,s}}^{x_{0,2}} \sim \sum_{j=1}^{3} I_{k=1}^{(j)}, \tag{17}$$

where the components $x_{0,1}$ (= 0) and $x_{0,2}$ [$= (2s+3)\pi/4$] correspond to the positions of the end points of the first peak ($k = 1$). The various subintegrals $I_{k=1}^{(j)}$ are also evaluated by assuming a constant value of the distribution function and using the triangle integral method, similarly to the relation Eq. (15). The constant values are taken to be those evaluated at the midpoints of the first interval $[x_{0,1},x_{1,s}]$ and last interval $[x_{2,s},x_{0,2}]$, while in the central region $[x_{1,s},x_{2,s}]$ the constant value is taken to be the maximum value of the distribution function located at $x_{1,s}$. It may be noted that the approximation of the distribution function in the central region can also be alternatively chosen to correspond to the midpoint value. However, the error in the latter approximation was found to be much higher (perhaps due to the rapid decay of the distribution function) and hence this alternative is not used.

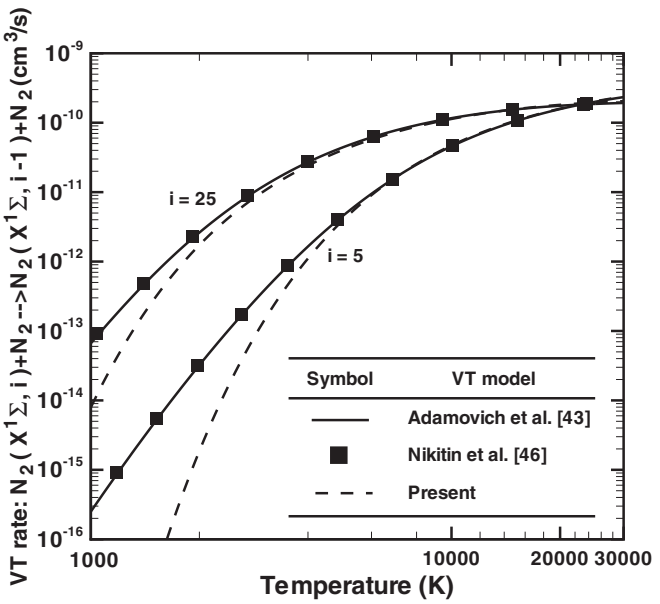

FIG. 2. Monoquantum VT rate coefficients related to $N_2(X\,^1\Sigma, i = 5,25) + N_2 \rightarrow N_2(X\,^1\Sigma, i-1) + N_2$ processes as functions of the translational temperature. Various VT models are considered.

The rate coefficients related to VT monoquantum transitions $N_2(X\,^1\Sigma, i) + N_2 \rightarrow N_2(X\,^1\Sigma, i-1) + N_2$ at low ($i = 5$) and higher ($i = 25$) quantum numbers are shown in Fig. 2. We can see that the asymptotic model of Nikitin and Osipov [46] agrees well with that of Adamovich *et al.* [43] in a wide range of temperature and vibrational states. The approximate model Eq. (16) of this study underestimates VT rate coefficients at low temperatures due to the simple quadrature calculation on the first peak ($I_{k=1}$). However, results obtained with this model become in very good agreement with those of FHO models from nearly 8000 K. Indeed, we saw that the distribution function covers more peaks ($k > 1$) at higher temperature, so quadrature calculations on these peaks are more accurate due to their narrowness. Figure 3 confirms that the rate coefficients of monoquantum VT transitions Eq. (16) developed in this study can be used for high temperatures and in the whole range of vibrational levels.

Figure 4 illustrates VT multiquantum and monoquantum rate coefficients from the 30th vibrational level to lower states i (=20,28,29) of the N_2 molecules in their ground electronic state $X\,^1\Sigma$. We can see that the multiquantum jumps predicted by Adamovich *et al.* [43] are in good agreement with those given by the model of Nikitin and Osipov [46], so that from now only this latter reference is considered for the comparison. The approximate model Eq. (16) developed in this study provides a very good agreement of the rate coefficients

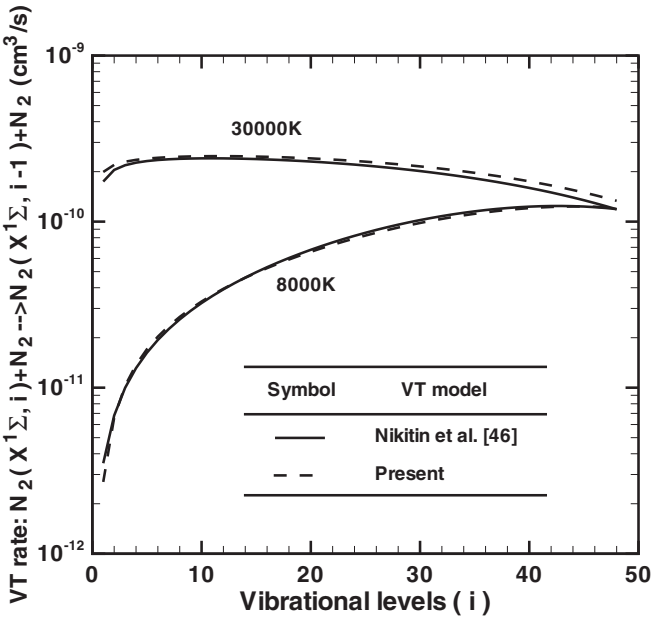

FIG. 3. Monoquantum VT rate coefficients related to $N_2(X\,^1\Sigma,i) + N_2 \rightarrow N_2(X\,^1\Sigma,i-1) + N_2$ processes for various temperatures (8000 and 40 000 K) and as functions of the vibrational quantum numbers i. Various VT models are considered.

with those given by the FHO models for temperatures over ~8000 K.

Note that multiquantum rate coefficients (i = 20,28) become comparable to that of the monoquantum process (i = 29) with rising translational temperature. Hence, multiquantum processes cannot be ignored in high temperature conditions. However, large multiquantum transitions (i = 20) are very unlikely to occur at lower temperature since collision

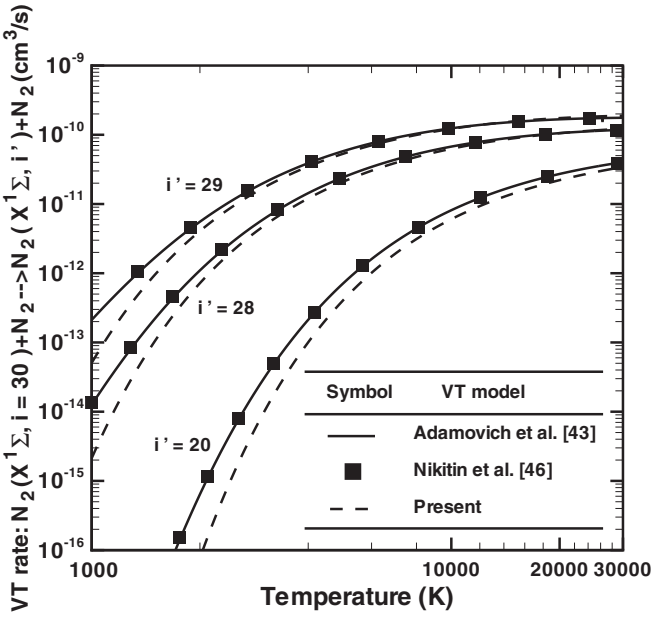

FIG. 4. Multiquantum and monoquantum VT rate coefficients related to $N_2(X\,^1\Sigma,i = 30) + N_2 \rightarrow N_2(X\,^1\Sigma,i' = 20,28,29) + N_2$ processes and as functions of the translational temperature. Various VT models are considered.

energies are not high enough to permit large energy jumps. Nevertheless, we can see in Fig. 4 that the rate coefficient for multiquantum transitions (i = 28) is not far from that of the monoquantum transition (i = 20) at low temperature. Indeed, since the energy levels become closer to each other with rising vibrational quantum numbers, the vibrational jumps become easier at moderate and high vibrational levels. Therefore, we can expect from Fig. 4 that the first vibrational levels are populated mainly by monoquantum transitions and thus the well known SSH model [37] can be applied for these levels at low temperature.

IV. APPLICATION AND DISCUSSION

Similarly to the works in Refs. [15–17,29,44], we consider a state-to-state nonequilibrium reactive gas flow, on the basis of kinetic equations for distribution functions in the spatial and temporal coordinates ($\mathbf{r},t$). The gas flow is under the following conditions:

$$\tau_{el} \sim \tau_{RR} \sim \tau_{RT} \ll \tau_{VT} \sim \tau_{VE} \sim \vartheta, \tag{18}$$

where $\tau_{el},\tau_{RR},\tau_{RT},\tau_{VT}$, and τ_{VE} are the characteristic mean times related to elastic, rotation-rotation (RR), rotation-translation (RT), vibration-translation (VT), and vibration-electronic (VE) processes; ϑ is the mean time of variation of macroscopic parameters. The above condition is satisfied in a wide temperature range, in particular for high enthalpy and high temperature hypersonic flows [1]. Under these conditions and using the modified Chapman-Enskog method [29,50,51], the zero-order distribution function of diatomic molecules is found to be in the following form:

$$f^{(0)}_{\alpha,i,j} = \left(\frac{m}{2\pi kT}\right)^{3/2} \frac{N_{\alpha,i}\, s^{\alpha i}_j}{Z^{\rm rot}_{\alpha,i}} \exp\left(-\frac{mC^2}{2kT} - \frac{\varepsilon^{\alpha i}_j}{kT}\right), \tag{19}$$

where m and k are the mass of the molecule and the Boltzmann constant, respectively. The terms $s^{\alpha i}_j$, $\varepsilon^{\alpha i}_j$, and $Z^{rot}_{\alpha,i}$ are the rotational statistical weight, the energy of the rotational level j, and the rotational partition function, respectively. These terms are related to the electrovibrational state (α,i) of the number density $N_{\alpha,i}$. The peculiar velocity $\mathbf{C}(=\mathbf{u}-\mathbf{v})$ is related to the macroscopic velocity $\mathbf{v}$ of the gas flow ($\mathbf{u}$ is the microscopic velocity of molecules). The molecular distribution Eq. (16) describes a local Maxwell-Boltzmann distribution over velocities and rotational energies at the gas temperature T. The nonequilibrium character of the gas flow is carried by the electrovibrational density $N_{\alpha,i}$.

The molecular distribution function Eq. (19) is expressed in terms of the macroscopic parameters $N_{\alpha,i}(\mathbf{r},t)$, $\mathbf{v}(\mathbf{r},t)$, and $T(\mathbf{r},t)$ which form a reduced set of variables to provide a closed self-consistent gas flow description in the state-to-state approach. A system of governing equations for these variables was derived in the general form in Refs. [15,29]. In the Euler approximation of a one-dimensional stationary gas flow behind a shock, this system of equations leads to the conservation equations of momentum and total energy coupled to the equations of state-to-state vibrational-electronic kinetics [16,17]:

$$\frac{d(vN_{\alpha,i})}{dx} = R_{\alpha,i}, \tag{20}$$

$$\rho v\frac{dv}{dx}+\frac{dP}{dx}=0, \tag{21}$$

$$\rho v\frac{dU}{dx}+P\frac{dv}{dx}=0, \tag{22}$$

respectively. The terms x, v, P, and U are the distance from the shock front, the flow velocity in the x direction, the pressure, and the total internal energy per unit mass, respectively. The source term in Eq. (20) is expressed as a sum of several source terms related to various processes:

$$R_{\alpha,i}=R^{VT}_{\alpha,i}+R^{VE}_{\alpha,i}. \tag{23}$$

The source term related to VT transitions is given by

$$R^{VT}_{\alpha,i}=\sum_M N_M\sum_{i'\neq i}\left(k^M_{\alpha,i'i}N_{\alpha i'}-k^M_{\alpha,ii'}N_{\alpha i}\right), \tag{24}$$

where the term N_M corresponds to the number density of the collisional partner M in the process Eq. (1). The forward rate coefficients $k^M_{\alpha,ii'}$ are calculated from the general form Eq. (5) by considering various VT models discussed in this paper. The backward rate coefficients $k^M_{\alpha,i'i}$ are obtained from the detailed balance at thermal equilibrium.

A VE transition can be described as follows:

$$A_{\alpha,i}+M\leftrightarrow A_{\alpha',i'}+M, \tag{25}$$

where the molecule A in its initial electronic state α is found in a final electronic state α'. The molecule is assumed to remain in the ground vibrational level of the corresponding electronic state ($i=i'=0$). The source term associated with this VE transition is

$$R^{VE}_{\alpha,i}=\sum_M N_M\sum_{\alpha'\neq\alpha}\left(k^M_{\alpha'}N_{\alpha'i'}-k^M_{\alpha}N_{\alpha i}\right), \tag{26}$$

where the rate coefficients k^M_{α} and $k^M_{\alpha'}$ expressed in the Arrhenius form are taken from Losev and Yarygina [52] for N_2 molecules.

We apply the governing equations (20), (21), and (22) to study a pure N_2 gas flow behind a plane shock wave. The ground $X\,^1\Sigma$ and first excited electronic states $A\,^3\Sigma$ and $B\,^3\Pi$ of N_2 molecules are considered in the modeling. These excited electronic states come from the VE transitions as follows [52]:

$$N_2(X\,^1\Sigma)+M\leftrightarrow N_2(A\,^3\Sigma,B\,^3\Pi)+M. \tag{27}$$

Coefficients of Dunham given in Refs. [53,55] are taken into account to calculate the vibrational energy levels of N_2 molecules in their various electronic states. These coefficients lead to 49, 31, and 29 total vibrational levels for $X\,^1\Sigma$,$A\,^3\Sigma$, and $B\,^3\Pi$ states, respectively. The free stream conditions are the same as in Ref. [56], i.e., a Mach number of 19.83, a temperature of 300 K, and a pressure of 27 Pa. Indeed, we expect in the future to complete the two-dimensional hypersonic blunt body N_2 gas flow simulations by Josyula *et al.* [56] using the analysis of results obtained in this paper.

Our N_2 gas flow is simulated on a 2 GHz quad-core Intel Xeon processor, by considering a geometric progression of ~80 000 grids along the x axis. Numerical calculations run until a distance of 10 cm behind the shock is reached. The stiff ordinary differential equations (20), (21), and (22) are integrated by using Gear's method [57].

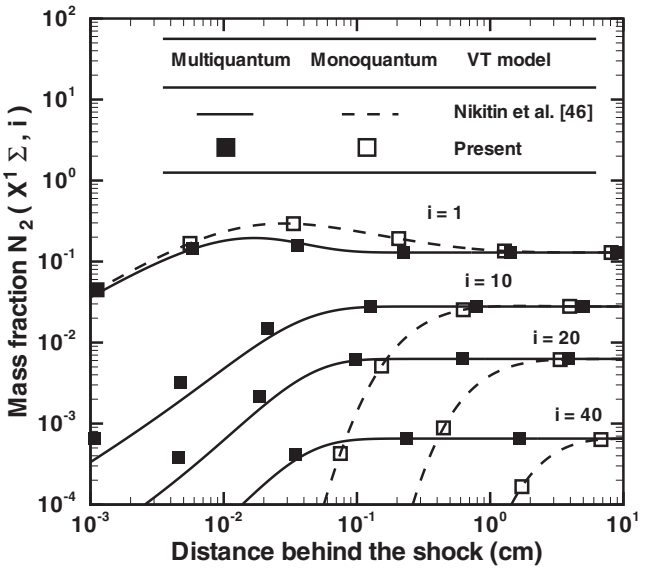

FIG. 5. Vibrational distributions of $N_2(X\,^1\Sigma,i=1,10,20,40)$ molecules as functions of the distance behind the shock. Multiquantum and monoquantum transitions and various VT models are considered. Free stream conditions: $P_\infty=27$ Pa, $T_\infty=300$ K, and $M_\infty=19.82$.

Figure 5 shows the vibrational distributions of molecules $N_2\left(X\,^1\Sigma,i\right)$ for various levels i (=1,20,30,40) as functions of the distance behind the shock. Compared to monoquantum transitions, those multiquantum transitions lead to a much faster relaxation of high vibrational states. Indeed, multiquantum mechanisms are more efficient on high levels because of their proximity to each other, so there is a small energy gap for the energy exchanges. Consideration of multiquantum processes causes a slight decrease of the concentration of the first vibrational states and more population of higher levels. Note that results obtained with the VT model of this study, Eq. (16), are in a good agreement with those obtained with the model of Nikitin and Osipov [46]. However, we can see in Table I that with the approximate model the one-dimensional N_2 gas flow code runs ~82 and ~107 times faster in cases of multiquantum and monoquantum collisions, respectively.

The local vibrational temperatures of each level i are illustrated in Fig. 6 and are defined as follows:

$$T^\alpha_v(i)=\frac{\left(\varepsilon^\alpha_i-\varepsilon^\alpha_{i=0}\right)}{k\ln(N_{\alpha,i}/N_{\alpha,i=0})}, \tag{28}$$

where the term ε^α_i corresponds to the energy of the vibrational level i related to the electronic state α. This figure confirms faster relaxation of high levels when multiquantum jumps are considered. Indeed, the vibrational temperatures of these states increase more rapidly with the distance from the shock compared to those of lower levels. In the case of monoquantum jumps, the behavior of these vibrational temperatures is opposite. Here, vibrational temperatures of high levels increase more slowly compared to those of lower states, because monoquantum processes involve vibrational energy exchanges only between nearest neighbor vibrational levels. Clearly, molecules reach a vibrational state by jumping step by step from the lower levels, which leads necessarily to a slower

TABLE I. Computing time estimated according to the various VT models, kind of vibrational energy exchange (monoquantum and multiquantum), and total number of vibrational levels in the modeling.

Energy exchange + electronic state	VT model	Clock time
Multiquantum + ground electronic state (49 levels)	Nikitin and Osipov [46]// Present	5.9 h// 4.3 min
Monoquantum + ground electronic state (49 levels)	Nikitin and Osipov [46]// Present	25 min// 14 s
Multiquantum + ground and excited electronic states (109 levels)	Nikitin and Osipov [46]// Present	1.8 days// 31.2 min
Monoquantum + ground and excited electronic states (109 levels)	Nikitin and Osipov [46]// Present	3.7 h// 2 min

relaxation of high levels in the case of monoquantum transitions. This kind of displacement through levels of vibration also explains the shift of the thermal equilibrium obtained with the various models of VT energy exchanges. Indeed, molecules need more VT collisions to reach a vibrational level on a characteristic time of observation, so these molecules reach the thermal equilibrium at a longer distance behind the shock than in the multiquantum case.

In this Fig. 6, we can also see that the translational temperature decreases more rapidly with the distance when we take into account multiquantum processes. This behavior arises from the rapid release of energy from the translational mode to the vibrational one resulting in the population of higher vibrational levels and allowing them a fast relaxation. Note that from the evolution of the translational temperature with the distance behind the shock, we can see that multiquantum processes become active when intermediate levels become sufficiently populated from the first levels. Indeed, molecules on these intermediate levels can easily jump to higher vibrational states since energy levels become closer to each other for higher vibrational quantum number, and multiquantum transitions are more efficient when energy gaps are small. Figure 6 also confirms the limits of application of one- and multitemperature models. These models assume a single vibrational temperature

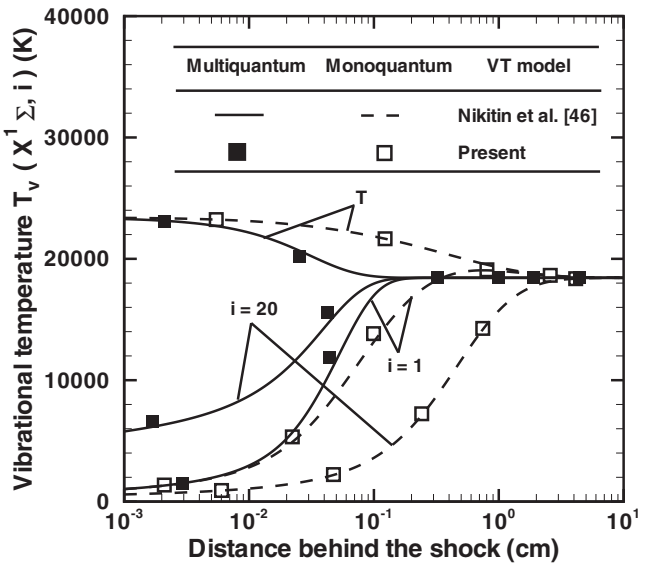

FIG. 6. Evolution of local vibrational temperatures of $N_2(X\,^1\Sigma, i = 1,20)$ molecules and the translational temperature as functions of the distance behind the shock. Multiquantum and monoquantum transitions and various VT models are considered. Free stream conditions: $P_\infty = 27$ Pa, $T_\infty = 300$ K, and $M_\infty = 19.82$.

for all levels, which is not the case in the figure as shown by the state-to-state approach.

Figure 7 illustrates the vibrational distribution as a function of the vibrational quantum number related to N_2 molecules in their ground electronic state. This figure is obtained by considering multiquantum and monoquantum processes for various distances behind the shock (0.01 and 0.03 cm). It is clear that multiquantum mechanisms populate intermediate and high levels more quickly, i.e., for $i > \sim 10$. With the multiquantum transition case, the last vibrational levels seem to follow a Boltzmann distribution with a common vibrational temperature. This can be explained by the fact that the energies of these last levels are so close (compared to lower levels) that a few VT collisions permit them to follow a similar relaxation behind the shock. However, concentrations of the first levels ($i <\sim 10$) vary and decrease slowly during the relaxation of the gas flow behind the shock wave. The reason for the slow variation is that VT transitions of molecules in the first vibrational levels require a large energy gap and monoquantum or multiquantum collisions are less effective in these conditions. The concentrations of the first vibrational levels decrease because molecules in these levels jump to higher levels due to VT transitions. This figure also shows that the VT model developed in this paper gives satisfactory results.

Figures 8, 9, and 10 present the vibrational temperature related to the first ($i = 1$), intermediate ($i = 20$), and last ($i = 40$) vibrational levels as a function of the distance behind the shock, calculated taking into account various VT energy exchanges. Monoquantum ($s = 1$) and multiquantum ($s > 1$) transitions are considered. These figures show that all vibrational levels are influenced by multiquantum processes. However, relaxation of the first vibrational levels is finally achieved by VT collisional interaction between the five nearest levels. Densities of intermediate and higher levels depend, respectively, on 20 and almost all levels (~40) of the ground electronic state. This behavior of all levels shows again the connection of the efficiency of multiquantum transitions with the magnitude of the energy jumps. Indeed, transitions from the first levels already occur for large energy jumps, so VT transitions are less efficient and only a few nearest levels contribute to multiquantum mechanisms. However, the energy levels are closer for higher quantum numbers of the vibration; therefore vibrational distributions of higher levels are sensitive to the concentrations of more levels via VT collisions. The above results show that the number of multiquantum transitions needed in our simulations to capture state-specific behavior increases with vibrational quantum number. This observation can be used to further improve the computational efficiency of our simulations by using different maximum

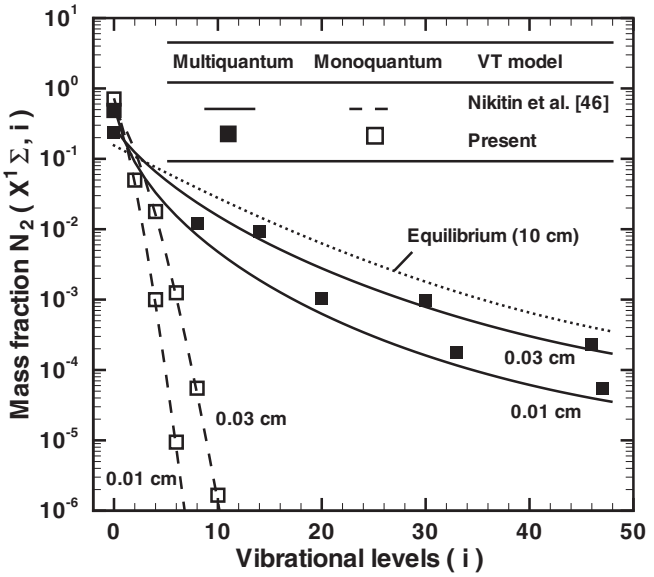

FIG. 7. Vibrational distributions of molecules $N_2(X\,^1\Sigma,i)$ as functions of the vibrational quantum number i for various distances behind the shock. Multiquantum and monoquantum transitions and various VT models are considered. Free stream conditions: $P_\infty =$ 27 Pa, $T_\infty = 300$ K, and $M_\infty = 19.82$.

numbers of allowable jumps depending on the vibrational quantum number of each state.

Figure 11 also shows the influence of VT processes on the evolution of the translational temperature with the distance behind the shock. We can see that this evolution is almost entirely governed by the first and intermediate vibrational levels. Indeed, the densities of higher levels are too weak compared to those of low levels, and thus they cannot play a great role in the evolution of the macroscopic parameters of the gas flow with the initial conditions of this study.

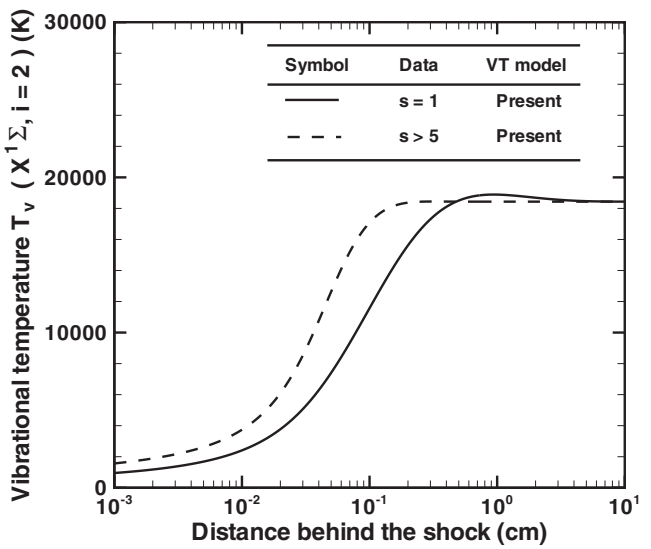

FIG. 8. Evolution of the local vibrational temperature of $N_2(X\,^1\Sigma,i = 1)$ molecules as a function of the distance behind the shock. Monoquantum ($s = 1$) and multiquantum ($s > 1$) transitions are considered. Free stream conditions: $P_\infty = 27$ Pa, $T_\infty = 300$ K, and $M_\infty = 19.82$.

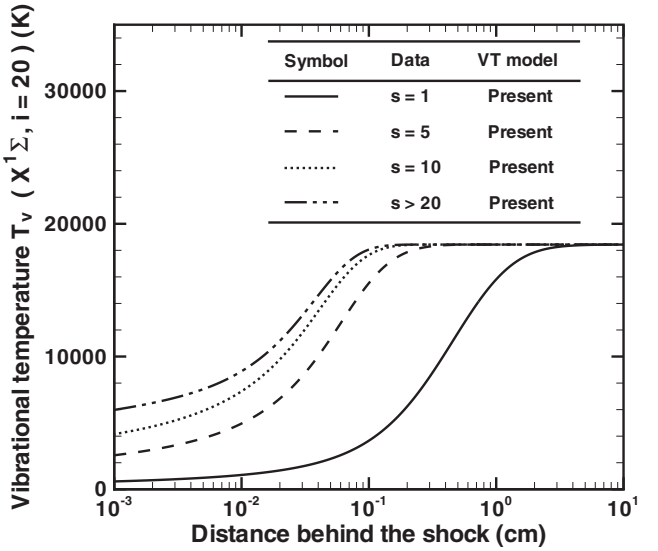

FIG. 9. Evolution of the local vibrational temperature of $N_2(X\,^1\Sigma,i = 20)$ molecules as a function of the distance behind the shock. Monoquantum ($s = 1$) and multiquantum ($s > 1$) transitions are considered. Free stream conditions: $P_\infty = 27$ Pa, $T_\infty = 300$ K, and $M_\infty = 19.82$.

Until now, only the ground electronic state of N_2 molecules was considered with its 49 total vibrational levels ($i = 0, \ldots, 48$). Now, the excited electronic states $A\,^3\Sigma$ and $B\,^3\Pi$ are implemented in the modeling and Fig. 12 shows their evolution with the distance behind the shock in consideration of various VT mechanisms and models. We can see that concentrations of excited electronic states still relax and do not reach the equilibrium state at a distance of under 10 cm. Moreover, their concentration is slightly higher in the case of monoquantum transitions because molecules

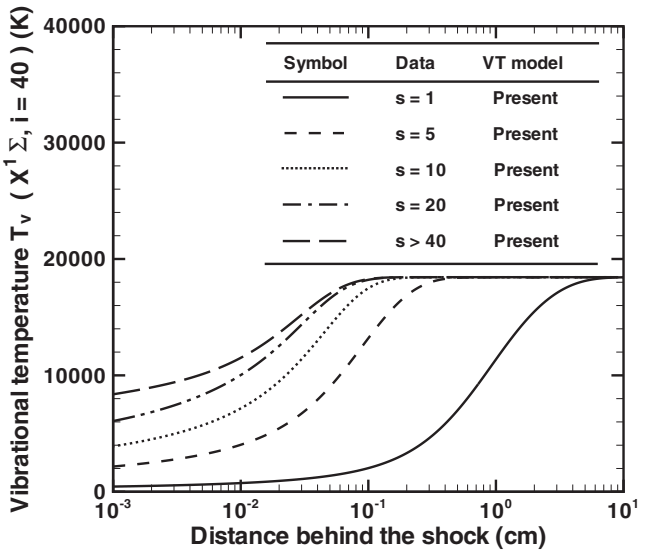

FIG. 10. Evolution of the local vibrational temperature of $N_2(X\,^1\Sigma,i = 40)$ molecules as a function of the distance behind the shock. Monoquantum ($s = 1$) and multiquantum ($s > 1$) transitions are considered. Free stream conditions: $P_\infty = 27$ Pa,$T_\infty = 300$ K, and $M_\infty = 19.82$.

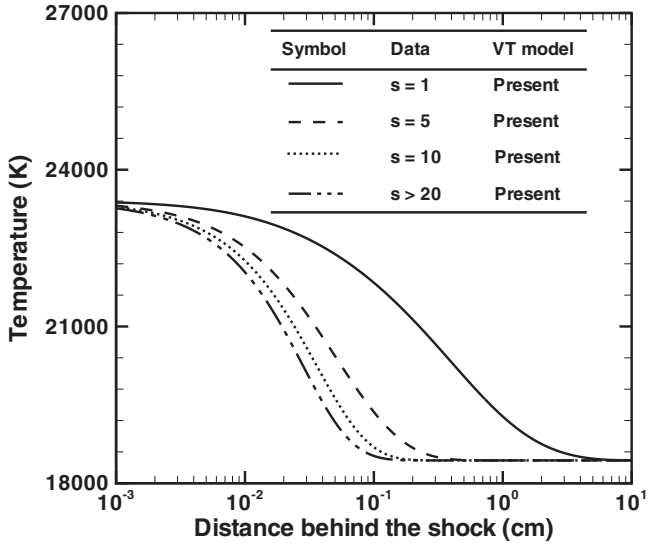

FIG. 11. Evolution of the translational temperature as a function of the distance behind the shock. Monoquantum ($s = 1$) and multiquantum ($s > 1$) transitions are considered. Free stream conditions: $P_\infty = 27$ Pa, $T_\infty = 300$ K, and $M_\infty = 19.82$.

reach excited electronic states via VE collisions [see Eq. (27)] from their first vibrational levels of the ground electronic state. Indeed, we saw above that populations of the first levels related to the ground electronic state are higher with monoquantum collisions (see Fig. 5).

However, as the total mass fraction is equal to unity, we can see that the densities of the excited electronic states remain very low under the free stream conditions of this study. Therefore, excited electronic states can be neglected in the actual modeling, and N_2 molecules in their ground electronic state give the main contribution to the predicted evolution of the gas flow macroscopic parameters. Nevertheless, these excited electronic states must be taken into account if radiative intensities from the first positive N_2 system [58] are expected to be evaluated accurately. Note that vibration-electronic transitions observed for CO molecules [59,60] may effectively increase the concentration of excited electronic levels in the present modeling. Unfortunately, data for VE jumps related to N_2 molecules are not available to our knowledge. Figure 12 also shows the good agreement of electronic level concentrations obtained using the present VT model with that of Nikitin and Osipov [46].

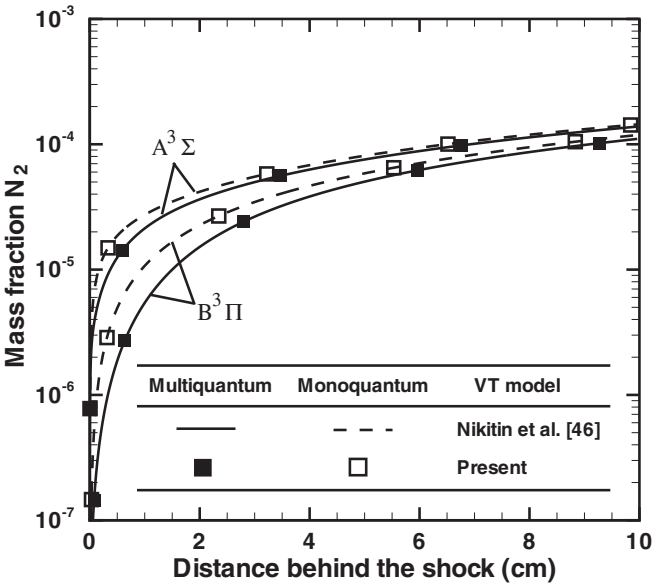

FIG. 12. Evolution of concentrations of N_2 molecules in their excited states $A^3\Sigma$ and, $B^3\Pi$ as functions of the distance behind the shock. Multiquantum and monoquantum transitions and various VT models are considered. Free stream conditions: $P_\infty = 27$ Pa, $T_\infty = 300$ K, and $M_\infty = 19.82$.

Further, it would be interesting to evaluate the increase in computing time required by the one-dimensional numerical code, when excited electronic states are considered along with supplemental vibrational levels. Indeed, the excited electronic states of N_2 molecules involve slightly more than double the total number of vibrational levels (=106). Table I shows that consideration of excited electronic states considerably increases the computing time with the VT model of Nikitin and Osipov [46]. Indeed, the latter model implies almost two days of computing time, whereas our model requires only about thirty minutes in the multiquantum case. When considering monoquantum transitions, the model developed in this study is also ~100 times faster.

V. CONCLUSIONS

A model is presented in this paper to calculate FHO rate coefficients related to VT transitions at high temperatures. This model is obtained with a quadrature method by using properties of Bessel's functions. Rates obtained with this model are in good agreement with those obtained with FHO models found in the literature. This model is used to simulate a pure N_2 gas flow behind a shock by considering a state-to-state approach. The macroscopic parameters behind the shock obtained using the proposed model are similar to those obtained on the basis of FHO models. The difference lies in the computing time, where the model developed in this study is ~100 times faster. For the free stream conditions considered in this work we found a low concentration of N_2 molecules in their excited electronic states; therefore they can be neglected in the modeling. Nevertheless, their presence shows that additional vibrational levels strongly increase the computing time especially if multiquantum transitions are taken into account. Multiquantum processes are found to have a great influence on the evolution of macroscopic parameters of the N_2 gas flow behind the shock. Indeed, the relaxation of high vibrational states is much faster than that of lower states, while a contrary behavior is observed if monoquantum transitions are considered. Moreover, with multiquantum processes, a thermal equilibrium distribution of vibrational levels is attained at a considerably shorter distance behind the shock. Multiquantum jumps must be taken into account for all vibrational levels in modeling. However, the number of these transitions may decrease inversely as a function of the vibrational quantum numbers.

Further validation of the approximate model developed in this study can be performed using more accurate quantum calculations or experimental data on VT energy exchanges

at high temperatures. However, this model can be efficiently utilized in nonequilibrium gas flow studies, because it can allow us to consider excited electronic states of molecules and their multiquantum jumps with a very short computing time. We plan to extend the present work to investigate the effects of dissociation of N_2 molecules by accounting for VT multiquantum transitions obtained with the proposed model.

ACKNOWLEDGMENTS

E.J. gratefully acknowledges financial support from the US Air Force Office of Scientific Research (AFOSR). P.V. and A.A. gratefully acknowledge financial support from the US Air Force Research Laboratory (AFRL) and the High Performance Technologies Inc. (HPTi).

[1] M. Cacciatore, M. Capitelli, S. de Benedictis, M. Dilanardo and C. Gorse, in *Nonequilibrium Vibrational Kinetics*, edited by M. Capitelli (Springer-Verlag, Berlin, 1986).
[2] C. S. Wang Chang and G. Uhlenbeck, University of Michigan, Research Report No. CM-681, 1951 (unpublished).
[3] S. Pascal and R. Brun, Phys. Rev. E **47**, 3251 (1993).
[4] E. V. Kustova and E. A. Nagnibeda, in *Rarefied Gas Dynamics 19*, (Oxford Science Publications, Oxford, 1995), vol. 1.
[5] E. V. Kustova and E. A. Nagnibeda, Chem. Phys. **208**, 313 (1996).
[6] G. Billing and E. Fisher, Chem. Phys. **43**, 395 (1979).
[7] G. Billing and R. Kolesnick, Chem. Phys. Lett. **200**, 382 (1992).
[8] G. Billing, in *Nonequilibrium Vibrational Kinetics* (Ref. [1]), p. 85.
[9] F. Esposito and M. Capitelli, Chem. Phys. Lett. **418**, 581 (2006).
[10] F. Esposito, M. Capitelli, and C. Gorse, Chem. Phys. **257**, 193 (2000).
[11] F. Esposito and M. Capitelli, Chem. Phys. Lett. **302**, 49 (1999).
[12] E. Nagnibeda, in *Aerothermodynamics for Space Vehicles*, edited by J. Hunt (ESA Publication Division, ESTEC, Noordwijk, Netherlands, 1995).
[13] F. Lordet, J. Meolans, A. Chauvin, and R. Brun, Shock Waves **4**, 299 (1995).
[14] I. Adamovich, S. Macheret, J. Rich, and C. Treanor, AIAA J. **33**, 1064 (1995).
[15] E. V. Kustova, A. Aliat, and A. Chikhaoui, Chem. Phys. Lett. **344**, 638 (2001).
[16] A. Aliat, A. Chikhaoui, and E. V. Kustova, Phys. Rev. E **68**, 056306 (2003).
[17] A. Aliat, E. V. Kustova, and A. Chikhaoui, Chem. Phys. **314**, 37 (2005).
[18] S. Ruffin and C. Park, in *30th Aerospace Sciences Meeting* (American Institute of Aeronautics and Astronautics, Reno, NV, 1992), AIAA 92-0806.
[19] A. Chiroux de Gavelle de Roany, C. Flament, J. Rich, V. Subramanian, and W. Warren Jr., AIAA J. **31**, 119 (1993).
[20] B. Shizgal and F. Lordet, J. Chem. Phys. **104**, 3579 (1996).
[21] G. Colonna, M. Tuttafesta, M. Capitelli, and D. Giordano, in *Rarefied Gas Dynamics 21* (CEPADUES, Toulouse, France, 1999), vol. 2, p. 281.
[22] E. Josyula and W. F. Bailey, J. Thermophys. Heat Transfer **18**, 550 (2004).
[23] I. Armenise, M. Capitelli, G. Colonna, and C. Gorse, J. Thermophys. Heat Transfer **10**, 397 (1996).
[24] M. Capitelli, I. Armenise, and C. Gorse, J. Thermophys. Heat Transfer **11**, 570 (1997).
[25] E. Josyula, J. Thermophys. Heat Transfer **14**, 18 (2000).
[26] E. Josyula and W. F. Bailey, AIAA J. **41**, 1611 (2003).
[27] G. Candler, J. Olejniczak, and B. Harrold, Phys. Fluids **9**, 2108 (1997).
[28] E. V. Kustova and E. Nagnibeda, Chem. Phys. **233**, 57 (1998).
[29] E. V. Kustova and A. Chikhaoui, Chem. Phys. **255**, 59 (2000).
[30] J. Arnold, V. Reis, and H. T. Woodward, AIAA J. **3**, 2019 (1965).
[31] C. Park, in *Nonequilibrium Hypersonic Aerthermodynamics* (Wiley and Sons, New York, 1990).
[32] G. Candler and C. Park, in *AIAA Thermophysics, Plasmadynamics and Lasers Conference* (American Institute of Aeronautics and Astronautics, San Antonio, TX, 1988), AIAA 88-2678.
[33] I. Adamovich, S. Macheret, J. Rich, and C. Treanor, AIAA J. **33**, 1064 (1995).
[34] D. Secrest and B. Johnson, J. Chem. Phys. **45**, 4556 (1966).
[35] X. Chapuisat, G. Bergeron, and J. M. Launay, Chem. Phys. **20**, 285 (1977).
[36] X. Chapuisat, G. Bergeron, and J. M. Launay, Chem. Phys. **36**, 397 (1979).
[37] R. Schwartz, Z. Slawsky, and K. Herzfeld, J. Chem. Phys. **20**, 1591 (1952).
[38] B. Gordiets, A. Osipov, and L. Shelepin, in *Kinetic Processes in Gases and Molecular Lasers* (Gordon and Breach Science Publishers, Amsterdam, 1988).
[39] K. N. C. Bray, J. Phys. B **1**, 705 (1968).
[40] E. H. Kerner, Can. J. Phys. **36**, 371 (1958).
[41] C. Treanor, J. Chem. Phys. **43**, 532 (1965).
[42] A. Zeleckow, D. Rapp, and T. Sharp, J. Chem. Phys. **49**, 286 (1968).
[43] I. Adamovich, S. Macheret, J. Rich, and C. Treanor, AIAA J. **33**, 1064 (1995).
[44] A. Aliat, Ph.D. thesis, Université de Provence, France, 2002.
[45] M. Lino da Silva, V. Guerra, and J. Loureiro, J. Thermophys. Heat Transfer **21**, 40 (2007).
[46] E. Nikitin and A. Osipov, in *Kinetic and Catalysis* (VINITI, All-Union Institute of Scientific and Technical Information, Moscow, 1977), vol. 4, Chap. 2 (in Russian).
[47] L. Landau and E. Teller, Phys. Z. Sowjetunion **10**, 34 (1936).
[48] K. Balla, O. S. Guk, and M. Vicsek, Comput. **50**, 77 (1993).
[49] N. Dyson, *Chromatographic Integration Methods* (Royal Society of Chemistry, Cambridge, 1992).
[50] E. Nagnibeda and E. Kustova, *Kinetic Theory of Transport and Relaxation Processes in Nonequilibrium Reacting Gas Flows* (Saint Petersburg University Press, Saint Petersburg, 2003).
[51] A. Chikhaoui, J. Dudon, E. Kustova, and E. Nagnibeda, Physica A **247**, 526 (1997).
[52] S. A. Losev and V. N. Yarygina, Russ. J. Phys. Chem. B **3**, 641 (2009).
[53] S. Edwards, J. Y. Roncin, F. Launay, and F. Rostas, J. Mol. Spectrosc. **162**, 257 (1993).

[54] F. Roux and F. Michaud, Can. J. Phys. **68**, 1257 (1990).
[55] Y. Babou, P. Riviere, M. Y. Perrin, and A. Soufiani, Int. J. Thermophys. **30**, 416 (2009).
[56] E. Josyula, W. F. Bailey, and C. J. Suchyta, in *47th AIAA Aerospace Sciences Meeting including the New Horizons Forum and Aerospace Exposition* (American Institute of Aeronautics and Astronautics, Orlando, FL, 2009), AIAA 2009-1579.
[57] C. W. Gear, *Numerical Initial Value Problems in Ordinary Differential Equations* (Prentice-Hall, Englewood Cliffs, NJ, 1971).
[58] C. O. Laux and C. H. Kruger, J. Quant. Spectrosc. Radiat. Transfer **48**, 9 (1992).
[59] R. L. DeLeon and J. W. Rich, Chem. Phys. **107**, 283 (1986).
[60] E. Plönjes, P. Palm, J. W. Rich, I. V. Adamovich, and W. Urban, Chem. Phys. **279**, 43 (2002).